ChemComm

COMMUNICATION

View Article Online
View Journal | View Issue

Cite this: *Chem. Commun.*, 2023, 59, 4475

Received 10th December 2022,
Accepted 16th March 2023

DOI: 10.1039/d2cc06736f

rsc.li/chemcomm

Liquid and solid-state tunable fluorescent carbon dots for trace water detection†

Nan Li, ‡[ab] Xuezhe Dong, ‡[ab] Xugui Lv, [ab] Yunfei Li, [b] Qingyu Ma, *[a] Ruifang Guan *[a] and Zheng Xie *[b]

We synthesized a type of sulfur and nitrogen co-doped carbon dot, which can achieve tunable fluorescence both in solutions and solid matrices, that is dominated by the surface state. Moreover, it can be used to detect trace water in a variety of organic solvents, especially in acetone with a limit of detection as low as 0.042%.

Carbon dots (CDs) are a type of emerging class of environment-friendly carbon-based luminescent nanomaterial with excellent optical properties, excellent biocompatibility and low toxicity.[1–5] These excellent properties make carbon dots show great application prospects in many fields, such as sensing, optoelectric devices, biological imaging, drug delivery and energy-related fields.[6–11] However, the fluorescence modulation mechanism of carbon dots is still unclear, which has puzzled researchers for a long time and limited the development of carbon dots to a certain extent. At present, various possible fluorescence mechanisms have been reported including the surface state, conjugation effect, synergistic effect, environment effect, crosslink-enhanced emission effect, and molecular state.[12]

Surface-state dominated fluorescence emission has been confirmed by a growing body of work in recent years, which leads to a variable fluorescence emission of carbon dots with the environment or the type and quantity of surface functional groups. Lyu *et al.*[13] introduced a pre-oxidation hydrothermal process to achieve tunable fluorescence emission from blue to red by modulating the relative content of nitrogen-containing functional groups on the surface. Bao *et al.*[14] prepared a series of carbon dots exhibiting various colors of fluorescence by varying their degree of surface oxidation or their size.

As a common phenomenon in the surface state, fluorescence emission influenced by the interaction between carbon dots and the environment has been reported by several groups, but the reason is still unclear. Khan and members of his research group found that the excitation wavelength-dependence of the carbon dots was affected by the slow relaxation between the carbon dots and the solvent molecules.[15] Kundu's team studied carbon dots with solvent-dependent properties based on *p*-phenylenediamine and citric acid systems and found that their fluorescence properties are related to the hydrogen bonding to the receptor capacity of the solvent environment.[16] Although many theoretical models have been used to explain the solvent-dependent fluorescence emission from carbon dots, there is still a need for a more in-depth understanding of such solvent-dependent mechanisms, and it is hoped that a new route for the preparation of tunable fluorescence carbon dots will be developed based on this and extended to the field of solid-state tunable fluorescence.

In this work, we used a simple one-step solvothermal treatment (Scheme 1) by selecting L-arginine and *o*-phenylenediamine as precursors and sulfuric acid as a solvent to obtain carbon dots, which were named as O-CDs. It has a broad spectrum of tunable fluorescence in different solvents and can achieve fluorescence changes from green to red, which shows that O-CDs have tunable fluorescence in the liquid state. Moreover, by doping the carbon dots with six different polymer substrates, solid-state films and gel

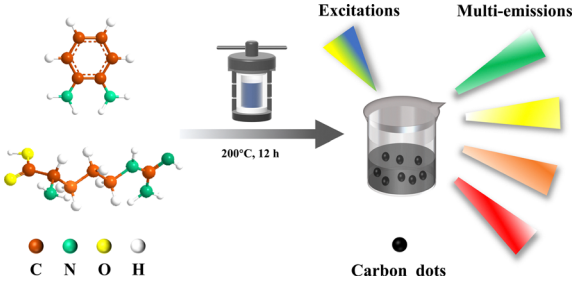

Scheme 1 Schematic illustration of the synthesis and multi-emission of carbon dots.

[a] *School of Materials Science and Engineering, University of Jinan, Jinan 250022, China. E-mail: mse_maqy@ujn.edu.cn, mse_guanrf@ujn.edu.cn*
[b] *Key Laboratory of Photochemical Conversion and Optoelectronic Materials, Technical Institute of Physics and Chemistry, Chinese Academy of Sciences, Beijing 100190, China. E-mail: zhengxie@mail.ipc.ac.cn*

† Electronic supplementary information (ESI) available. See DOI: https://doi.org/10.1039/d2cc06736f

‡ These authors contributed equally to this work.

glasses with different luminescence properties were prepared to achieve solid-state tunable fluorescence, demonstrating its potential for application in solid-state lighting. According to its polarity dependent properties, it can be used to detect trace water in organic solvents, with a lower limit of detection and good visualization under UV light compared to other carbon dots.

As shown in Fig. 1, the particle size of O-CDs was about 1.8 ± 0.6 nm, with a single particle dispersion, which was uniformly dispersed in the field of view. The HRTEM of it shows obvious lattice stripes, with a lattice spacing of about 0.21 nm and 0.24 nm, corresponding to the (100) facet of graphite.[17] The height of O-CDs is obtained from AFM, which is approximately 0.6–0.81 nm for the thickness of 1–2 layers of graphene. In the XRD spectrum (Fig. S1, ESI†), a characteristic diffraction peak at 24.3° was observed, corresponding to the (002) facet of graphite. The Raman spectrum (Fig. S2, ESI†) showed the D-band at 1378 cm^{-1} and the G-band at 1554 cm^{-1} with a two-peak intensity ratio of I_D/I_G being 1.02, indicating that O-CDs have a large degree of graphitization and more defects.[18] The results demonstrate that the precursors underwent a more thorough carbonization process in an autoclave.

Fourier transform infrared spectroscopy (FT-IR) of the raw materials o-phenylenediamine, L-arginine and O-CDs were tested separately and the results are shown in Fig. 1d. The broad peaks at 3439 cm^{-1} in the spectrum of O-CDs are attributed to the stretching vibrations of secondary amines and hydroxyl groups. The peak located at 767 cm^{-1} is attributed to the bending vibration in the adjacent double substitution plane of the benzene ring. In addition, the C=O stretching vibration at 1627 cm^{-1} and the N–H stretching vibration peak at 1589 cm^{-1} together demonstrate the generation of amide bonds. The XPS result in Fig. 1e shows four typical peaks at 167 eV (S 2p), 285 eV (C 1s), 399 eV (N 1s), and 530 eV (O 1s), demonstrating the successful doping of sulfur and nitrogen elements. As shown in Fig. 1f–i, by the high-resolution XPS spectra, the existence forms of the various elements were attributed to the split-peak fit, respectively. From the analysis results, it can be seen that carbon exists mainly as O=C–OH (288.5 eV), C=O/C=N (286 eV), C–N/C–S/C–O (285.1 eV) and C–C/C=C (284.6 eV). Nitrogen is mainly present in the form of pyrrole nitrogen (401.3 eV), amino nitrogen (400 eV) and pyridine nitrogen (398.6 eV). Oxygen exists mainly in the two forms of C–O (533 eV) and C=O (531.3 eV). Sulfur is present in different valence states in addition to C–SO_x–C (x = 2, 3, and 4). The percentages of each element in O-CDs are shown in Table S1, ESI,† and the percentages of each element present in the form are shown in Tables S2–S4, ESI.† The FT-IR and XPS results together demonstrate that the precursors generate carbon dots with various functional groups through an amidation reaction and carbonization. These functional groups give the carbon dots excellent dispersion in organic solvents, enabling them to achieve outstanding fluorescence properties in the solution state.[19]

O-CDs were dispersed in DMF and the optical properties of them were investigated using UV-Vis absorption spectra and PL and PLE spectra, as shown in Fig. 2a. The UV-Vis absorption spectra showed two intense peaks at 268 nm and 289 nm in the UV region, as well as a broad absorption peak centered at 500 nm in the visible region, which were attributed to the π–π* transition of the C=C bond and the n–π* transition of the C=N, C–N, C=O and C–O bonds, respectively.[17] The optimal excitation wavelength of O-CDs was 480 nm and the PL spectrum showed the emission located at 586 nm. The fluorescence result corresponds to the color coordinates (0.54, 0.46) of the Commission Internationale de l'Eclairage (CIE) (Fig. S3, ESI†), which proves that O-CDs have orange-red fluorescence emission. Meanwhile, Fig. 2b shows the emission independent of

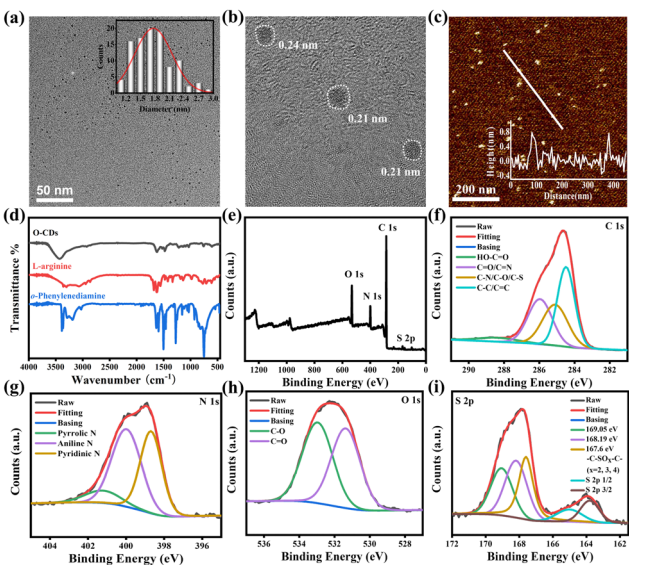

Fig. 1 (a) TEM and particle size distribution histogram. (b) HRTEM. (c) AFM and height statistics of O-CDs (d) FT-IR spectra. (e) XPS pattern of O-CDs. (f–i) High-resolution XPS patterns of C 1s, N 1s, O 1s, and S 2p of O-CDs.

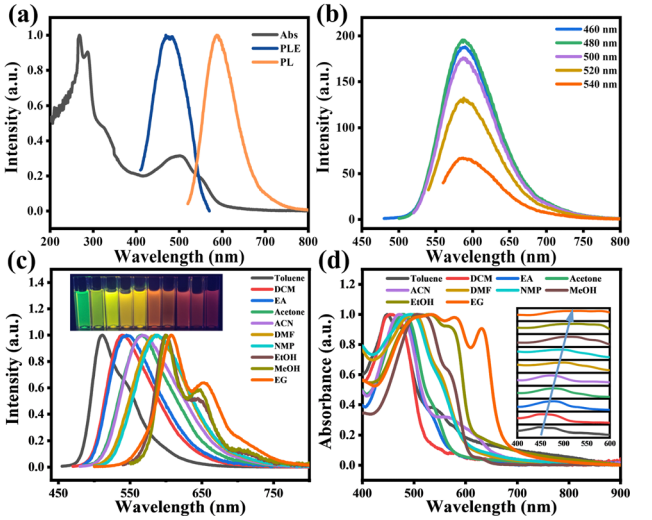

Fig. 2 (a) UV-vis absorption (black), PL (orange), and PLE (blue) spectra of CDs in DMF. (b) The PL spectra of CDs at different excitation wavelengths in DMF. (c) Normalized fluorescence spectra of O-CDs in different solvents. The inset shows photographs of O-CDs under UV light. (d) Normalized absorption spectra of O-CDs in different solvents. The inset shows the red-shift trend of the absorption peaks between 400 and 600 nm.

the excitation wavelength, demonstrating that there is no excitation-dependence of O-CDs, which is consistent with most of the previously reported carbon dots.[20–22] Fig. S4, ESI† shows that O-CDs have no concentration-dependence and possess good fluorescence stability (Fig. S5, ESI†) and excellent resistance to photobleaching (Fig. S6, ESI†).

Interestingly, we found that O-CDs possessed good solubility when dispersed in ten organic solvents and these solutions emitted bright green to red fluorescence under UV light, demonstrating the broad-spectrum tunable fluorescence properties of O-CDs. The normalized fluorescence spectra (Fig. 2c) showed that the emission peak gradually changed from 513 nm to 603 nm at a single excitation wavelength with the change of the solvent, which led to a variation in fluorescence color from green to red, and O-CDs exhibited emission independent of the excitation wavelength in each solvent (Fig. S7, ESI†). In the UV-Vis absorption spectrum (Fig. 2d), the different absorption bands from 447 nm red-shifted to 534 nm, indicating that O-CDs have different energy gaps in various solvents.[23] Plotting $E_T(30)$, which symbolizes the solvent polarity parameter, against the absorption peak and fluorescence peak of each solvent (Fig. S8, ESI†), it can be found that they have a good linear relationship. This can prove that the fluorescence color variation of carbon dots is mainly caused by the polarity of the solvent and the absorption and fluorescence peaks were gradually red-shifted with increasing solvent polarity. However, we found that when O-CDs were dissolved in alcohol solvents (ethanol, methanol, and ethylene glycol), although the polarity of these solvents increased sequentially, the UV-Vis absorption spectra and fluorescence spectra of O-CDs in these solvents changed insignificantly and differed from the phenomena in other solvents, such as the change from single-peak to double-peak emission and the wider absorption range. This may be due to the formation of hydrogen bonds between the O and N atoms on the surface of O-CDs and the hydroxyl groups of alcohols, which increase the stability of the excited states and lead to similar PL properties of O-CDs in alcohol solvents.[2,24]

We also investigated the absolute quantum yields (Fig. S9, ESI†) and fluorescence lifetimes (Fig. S10, ESI†) of O-CDs in a range of solvents. The results showed that O-CDs possessed high quantum yields in low-polarity solvents, with the highest quantum yield of 23.44% exhibited in ethyl acetate. All the fluorescence lifetimes fit a single exponential fit and exhibit similar fluorescence lifetimes of about 11 ns in their solvents except alcohol solvents, which exhibit about 7.35 ns in alcohol solvents. The lower quantum yields and fluorescence lifetimes in alcohol solvents may be due to the increase in hydrogen bonding that raises the internal conversion rate and vibrational relaxation, leading to a decrease in the radiative leap, which in turn leads to fewer photons emitted as fluorescence and subsequently to this result.[25] Furthermore, the absorption peaks in alcohol solvents are broad; this causes a lot of overlap between them and the emission peaks, which can result in self-absorption effects. These overlaps also reduce the quantum yield by transferring energy non-radiatively through electron interactions or by emitting and absorbing radiation.[26] The detailed parameters of O-CDs in different solvents are shown in Table S5, ESI.†

Most of the carbon dots in the aggregated state will produce the aggregation-caused quenching effect.[27] Based on our previous work[28] and the surface-state dominated fluorescence modulation properties of O-CDs, we effectively solved this problem by doping O-CDs into several different polymer matrices to construct solid-state PS, PMMA, PVP fluorescent films and MTES, GPTMS, and APTES-based gel glasses. The spectra and photographs of O-CDs in different substrates are shown in Fig. S11, ESI.† It can be clearly seen that the fluorescence peak is red-shifted from 511 nm in the PS film to 600 nm in the APTES-based gel glasses, achieving solid-state fluorescence modulation. The variation of the absorption spectra may be due to the lower doping of O-CDs and the effect of the polymer substrates. The solid-state luminescence of carbon dots on substrates under various doping concentrations and excitation wavelengths is shown in Fig. S12, ESI.† The fluorescence spectrum of each substrate shows a certain degree of red-shift with increasing carbon dot concentration, which should be attributed to the inevitable self-absorption phenomenon of the material.[29] The absolute quantum yields (Fig. S13, ESI†) and fluorescence lifetimes (Fig. S14, ESI†) of O-CDs doped in solid fluorescent films and gel glasses are both decreased compared to those in solvents. These may be due to two factors: first, that the dispersion of O-CDs within substrates is not completely uniform and there is still a certain degree of aggregation-caused quenching effect; second, that the polymer substrates may also absorb part of the energy, thus decreasing the absolute quantum yields and lifetimes too. The broad-band spectrum coverage of O-CD-doped solid-state fluorescent films and gel glasses provides a new idea in the field of solid-state lighting and has great application significance.

It is a key analytical method required in industry or research institutions to research various chemical processes by determining the trace water in organic solvents. At present, the determination of trace water in organic solvents is normally performed by the conventional Karl Fischer titration.[30] However, this method is complicated and uses toxic reagents. In the previous section, we have confirmed that O-CDs have surface state-dominated tunable fluorescence and polarity-dependence. Water is a highly polar liquid and its presence changes the polarity of the organic solvent, resulting in a significant increase in the polarity of the mixed solution. Based on this, we have developed a simple and efficient fluorescence technique to measure trace water content in organic solvents. Taking acetone as an example, we measured the fluorescence spectrum of O-CDs in an acetone/water mixed system with different water contents. As shown in Fig. 3a, with the water content in acetone raised from 0% to 10%, the fluorescence peak was red-shifted from 564 nm to 599 nm and the fluorescence intensity decreased to one-tenth of the original. The fluorescence color of the solution changed from bright yellow to orange under UV light (Fig. 3b), which indicated that O-CDs had good fluorescence visualization for the detection of water content in organic solvents. Fig. 3c and d show the results of the linear fit of the maximum emission peak and I_0/I of the solution to the water content in acetone. It can be seen that they have a good linear

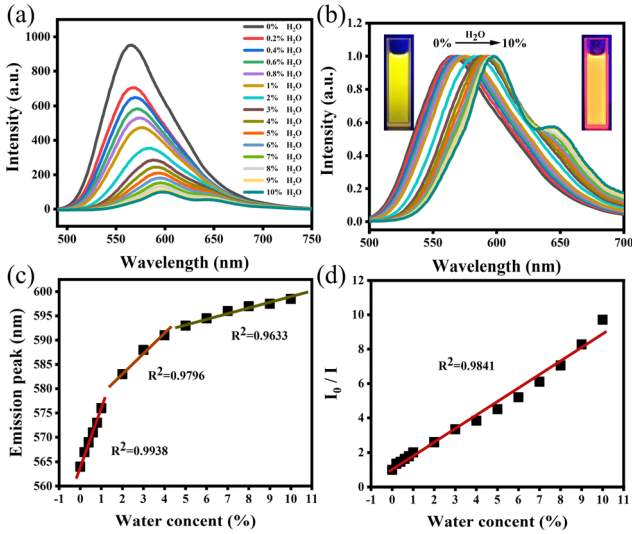

Fig. 3 (a) Fluorescence spectra of O-CDs in acetone with different water contents. (b) Normalized fluorescence spectra. Illustrations are photos of solutions with 0% and 10% water content under UV light. (c and d) Fitting of maximum emission peak and I_0/I.

relationship, especially in the 0–1% interval and the characteristic peaks and fluorescence intensity changes are very sensitive. The limit of detection (LOD) was 0.042% at a signal-to-noise ratio of 3. In addition to acetone, the water content can also be detected in other organic solvents such as acetonitrile and DMF (Fig. S15 and S16, ESI†). The limits of detection were 0.129% in acetonitrile and 0.132% in DMF. It can be seen from the results that O-CDs can detect trace water in organic solvents efficiently and sensitively, with lower LOD and more convenient operation compared with other CDs (Table S6, ESI†). It has excellent application prospects in the detection of trace water in organic solvents.

In summary, we prepared a type of carbon dot with surface-state dominantly tunable fluorescence by a one-step solvothermal method. It has high quantum yields, excellent time stability and resistance to photobleaching. These carbon dots can achieve a broad spectrum of tunable fluorescence from green to red in ten solvents. We attribute this solvent-dependent effect to the surface-state-dominated fluorescence modulation, including the effects of solvent polarity and hydrogen bonding, and we also successfully prepared a variety of O-CD-doped solid-state films and gel glasses with different substrates to achieve tunable solid-state fluorescence similar to that in solution, which provides a new solution for realizing solid-state lighting. Based on the high polarity sensitivity of O-CDs, the detection of trace water in organic solvents was achieved with low LOD and excellent application prospects.

The authors acknowledge financial support of the National Natural Science Foundation of China (No. 21875267).

Conflicts of interest

There are no conflicts to declare.

Notes and references

1 Y. Wu, J. Li, X. Zhao and X. Gong, *Carbon*, 2023, **201**, 796–804.
2 J. Ren, J. Sun, X. Sun, R. Song, Z. Xie and S. Zhou, *Adv. Opt. Mater.*, 2018, **6**, 1800115.
3 Q. Jia, J. Ge, W. Liu, X. Zheng, S. Chen, Y. Wen, H. Zhang and P. Wang, *Adv. Mater.*, 2018, **30**, e1706090.
4 Y. Xiong, J. Schneider, C. J. Reckmeier, H. Huang, P. Kasak and A. L. Rogach, *Nanoscale*, 2017, **9**, 11730–11738.
5 L. Wei, Y. Ma, X. Shi, Y. Wang, X. Su, C. Yu, S. Xiang, L. Xiao and B. Chen, *J. Mater. Chem. B*, 2017, **5**, 3383–3390.
6 L. Wang, M. Li, W. Li, Y. Han, Y. Liu, Z. Li, B. Zhang and D. Pan, *ACS Sustainable Chem. Eng.*, 2018, **6**, 12668–12674.
7 B. Yuan, S. Guan, X. Sun, X. Li, H. Zeng, Z. Xie, P. Chen and S. Zhou, *ACS Appl. Mater. Interfaces*, 2018, **10**, 16005–16014.
8 I. Milenkovic, M. Algarra, C. Alcoholado, M. Cifuentes, J. M. Lázaro-Martínez, E. Rodríguez-Castellón, D. Mutavdžić, K. Radotić and T. J. Bandosz, *Carbon*, 2019, **144**, 791–797.
9 L. Yang, Q. Su, B. Si, Y. Zhang, Y. Zhang, H. Yang and X. Zhou, *Chem. Eng. J.*, 2022, **429**, 132230.
10 S. Majumdar, G. Krishnatreya, N. Gogoi, D. Thakur and D. Chowdhury, *ACS Appl. Mater. Interfaces*, 2016, **8**, 34179–34184.
11 Y. Wang, L. Lu, H. Peng, J. Xu, F. Wang, R. Qi, Z. Xu and W. Zhang, *Chem. Commun.*, 2016, **52**, 9247–9250.
12 L. Ai, Y. Yang, B. Wang, J. Chang, Z. Tang, B. Yang and S. Lu, *Sci. Bull.*, 2021, **66**, 839–856.
13 B. Lyu, H.-J. Li, F. Xue, L. Sai, B. Gui, D. Qian, X. Wang and J. Yang, *Chem. Eng. J.*, 2020, **388**, 124285.
14 L. Bao, C. Liu, Z. L. Zhang and D. W. Pang, *Adv. Mater.*, 2015, **27**, 1663–1667.
15 S. Khan, A. Gupta, N. C. Verma and C. K. Nandi, *Nano Lett.*, 2015, **15**, 8300–8305.
16 A. Kundu, B. Park, J. Oh, K. V. Sankar, C. Ray, W. S. Kim and S. Chan Jun, *Carbon*, 2020, **156**, 110–118.
17 E. Shuang, Q. X. Mao, J. H. Wang and X. W. Chen, *Nanoscale*, 2020, **12**, 6852–6860.
18 M. Wu, J. Zhan, B. Geng, P. He, K. Wu, L. Wang, G. Xu, Z. Li, L. Yin and D. Pan, *Nanoscale*, 2017, **9**, 13195–13202.
19 X. Cui, Y. Wang, J. Liu, Q. Yang, B. Zhang, Y. Gao, Y. Wang and G. Lu, *Sens. Actuators, B*, 2017, **242**, 1272–1280.
20 A. Singh, Z. Qu, A. Sharma, M. Singh, B. Tse, K. Ostrikov, A. Popat, P. Sonar and T. Kumeria, *J. Nanostruct. Chem.*, 2022, DOI: **10.1007/s40097-022-00501-5**.
21 L. Shi, L. Li, X. Li, G. Zhang, Y. Zhang, C. Dong and S. Shuang, *Sens. Actuators, B*, 2017, **251**, 234–241.
22 Z. Han, K. Wang, F. Du, Z. Yin, Z. Xie and S. Zhou, *J. Mater. Chem. C*, 2018, **6**, 9631–9635.
23 J. H. Liu, Y. Li, J. H. He, D. Yuan, R. S. Li, S. J. Zhen, Y. F. Li and C. Z. Huang, *ACS Appl. Mater. Interfaces*, 2020, **12**, 4815–4820.
24 J. Bai, Y. Ma, G. Yuan, X. Chen, J. Mei, L. Zhang and L. Ren, *J. Mater. Chem. C*, 2019, **7**, 9709–9718.
25 Y. Sun, H. Qin, X. Geng, R. Yang, L. Qu, A. N. Kani and Z. Li, *ACS Appl. Mater. Interfaces*, 2020, **12**, 31738–31744.
26 A. P. Piquettea, M. E. Hannaha and K. C. Mishra, *ECS Trans.*, 2012, **41**(37), 1–9.
27 N. Wang, Z. X. Liu, R. S. Li, H. Z. Zhang, C. Z. Huang and J. Wang, *J. Mater. Chem. B*, 2017, **5**, 6394–6399.
28 Z. Xie, F. Wang and C. Y. Liu, *Adv. Mater.*, 2012, **24**, 1716–1721.
29 Y. Chen, M. Zheng, Y. Xiao, H. Dong, H. Zhang, J. Zhuang, H. Hu, B. Lei and Y. Liu, *Adv. Mater.*, 2016, **28**, 312–318.
30 K. Fischer, *Angew. Chem., Int. Ed. Engl.*, 1935, **48**, 394–396.

